ARKIV FÖR FYSIK Band 19 nr 5

Communicated 12 October 1960 by G. Borelius and K. Siegbahn

X-ray flash spectra of Fe, Ni and Cu

By Per Olof Schörling

With 15 figures in the text

ABSTRACT

K-spectra of Fe, Ni and Cu from an X-ray flash tube with low inductance have been recorded photographically and compared with spectra from an ordinary X-ray tube. In the flash spectrum the satellite $K\beta'$ was much stronger, the $K\alpha_1$ line was broadened on both sides, the $K\alpha_2$ line on the low energy side, and the $K\beta_{1,3}$ line on the high energy side. The probable cause of these effects is multiple ionization by successive collisions with incident cathode electrons. The results support Parratt's explanation of the origin of $K\beta'$ and the asymmetry of $K\alpha_1$ and $K\alpha_2$. An alternative theory by Kakuschadse is rejected.

1. Introduction

Most X-ray satellites are supposed to represent electron transitions in atoms with more than one inner vacany. Most L- and M-satellites undoubtedly arise from multiple ionization caused by the Auger effect. This is not true of K-satellites. It is probable that, occasionally, one single collision between the atom and one incident cathode electron leaves the atom in a state of multiple ionization. States produced in this way seem to be involved in K-satellite transitions. The probability of multiple ionization of the inner electron shells by *successive* electron impacts is normally too low [2]. This has been verified experimentally in different ways [3–6].

Professor Per Ohlin of this Institute proposed in 1956 that the effect of successive electron impacts might be measureable in the spectrum of an X-ray flash tube with very high current density. He also pointed out that especially high current density would be attained by lowering as much as possible the inductance of the discharge circuit. This has been done in the present work. K-spectra of Fe, Ni and Cu from the flash tube and from an ordinary X-ray tube have been recorded photographically and compared. The observed differences between the two types of spectra will be discussed.

2. Apparatus

2.1. *The spectrograph*

The spectrograph was constructed and described by Flemberg [7]. Fig. 1 is an extremely simplified sketch of the spectrograph. F is the centre of the focus spot of the X-ray tube and the X-ray flash tube, respectively. C is the centre of the reflecting curved crystal surface. P is the centre of the sensitive layer of the photographic

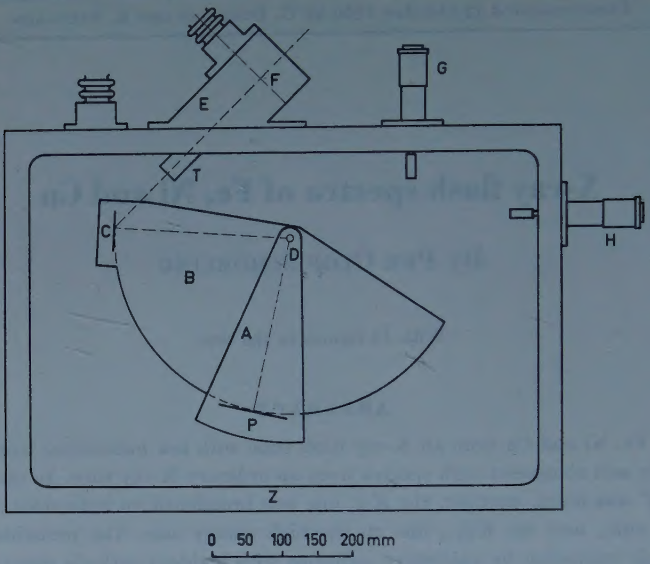

Fig. 1. Sketch of the spectrograph. The notations are explained in the text.

plate. A is a metal arm carrying the plate holder. A may be rotated round the axis D. B is a metal plate carrying the crystal table with the crystal holder. The system B + A may be rotated round the axis C. When the spectrograph is evacuated, this rotation is rendered possible by the arrangement G. CD is perpendicular to the crystal surface and PD is perpendicular to the photographic plate. When recording an X-ray line with Bragg angle θ, the spectrograph should be so adjusted that the angles FCD and CDP are equal to $90^\circ - \theta$ and 2θ, respectively. In addition the distances CD and PD should be equal to half the radius of curvature of the crystal face. CD and PD are variable, which makes it possible to fulfil this condition. FC may be given five different fixed values by displacing C. The arrangement H is used in order to raise and lower a shutter immediately in front of the photographic plate. Thus the X-ray spectrum and the X-ray flash spectrum to be compared are recorded above each other on the same plate. The tube T has on its front side, nearest to the crystal, a suitable rectangular opening covered with a thin aluminum foil. The foil protects the crystal from the metal evaporated from the flash tube anode. The spectrograph and the X-ray tube (flash tube) are evacuated via the two tombac tubes by means of a mechanical pump (Balzers Duo 5) and an oil diffusion pump (Balzers Diff 120 filled with Balzers Diff-Oel Nr. 7). The pressure is measured at Z with a Pirani gauge and an ionization gauge. The tube body E is earthed by a coarse multi-wired copper cable.

A more detailed description of the spectrograph is found in [7]. The crystal holder described there is not identical with the one used in the present investigation, but the differences are not essential.

The crystal used was a quartz one, $25 \times 15 \times 0.4$ mm^3. The reflecting plane was 1340 with $d_1 = 1177.61$ X.U.

The spectra were recorded on Ilford Process Plate N. 40, a plate material characterized by slow emulsion, high contrast and very fine grain.

2.2. *The X-ray tube*

The X-ray tube was described by Flemberg [7]. The PtIr filament heated by a current of 2.0 A gave an emission of about 3 mA. The voltage supplied by a Graetz-coupled high voltage set was smoothed by a 0.25 μF condenser. A 4 MΩ resistance in series with the X-ray tube prevented the condenser from flash-discharging through the tube.

2.3. *The X-ray flash tubes*

The discharge circuit consists of a condenser and a flash tube. Three such units have been used, with successively increased current density and increased integrated intensity per flash. They will be called units I, II and III, respectively. The same trigger system was used for them all. It is described in 2.4. The condensers were charged by the high voltage set via a resistance of between 2 and 30 MΩ. At all X-ray and X-ray flash exposures the voltage was measured with a micro-ammeter and a resistance of 102.44 MΩ.

The maximum current I_{max} during the discharge is

$$I_{max} \approx V_0 \cdot \sqrt{\frac{C}{L}} \tag{1}$$

where V_0 is the initial voltage of the condenser C, and L is the inductance of the circuit. A low value of L causes both high current density and high intensity of the

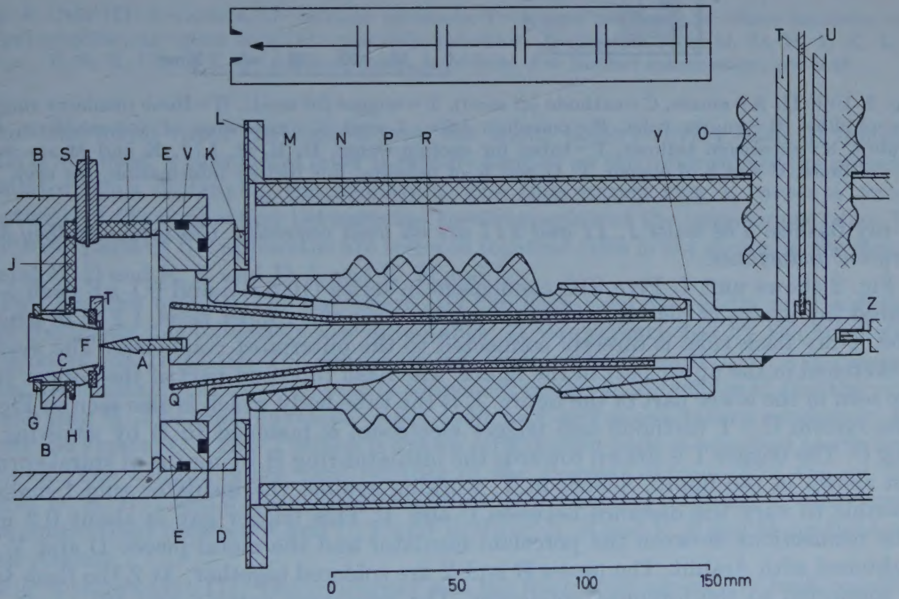

Fig. 2. Unit I. Above: sketch of the whole discharge circuit. Below: the X-ray flash tube. A = anode, C = cathode (of steel), T = trigger (of steel), H and I = insulator rings of steatite, S = sealed terminal, J and O = insulators of perspex, P = porcelain insulator, Q = glass tube, N = insulator tube of bakelite, V = rubber packing. B, E, G, D and Y are made of brass, K, L, M and R of copper. For further information, see text.

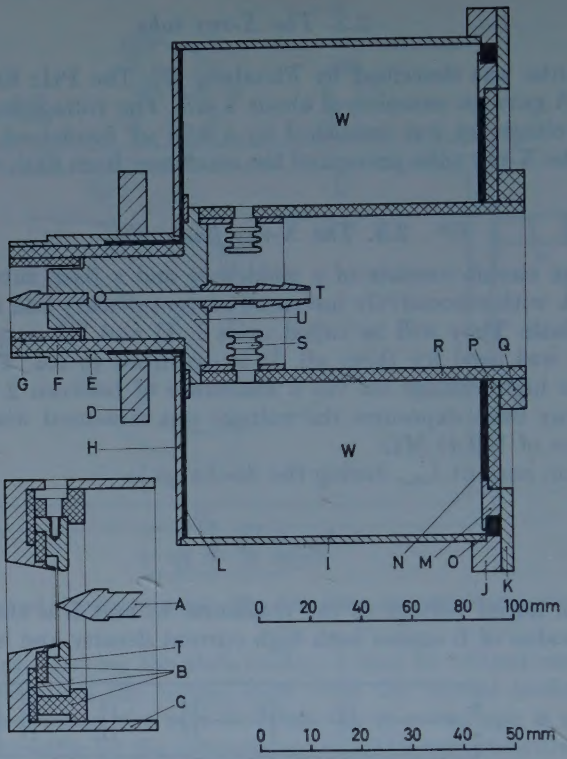

Fig. 3. Unit II. A = anode, C = cathode (of steel), T = trigger (of steel), B = three insulator rings of pyrophyllite, G = quartz tube, F = porcelain tube, L and N = insulators of polyethylene, O = Araldit, S = expansion bellows, T = tubes for cooling-water. D, E, H, I, J, K and M are made of brass, U and S of copper, P, Q and R of bakelite. For further information, see text.

X-ray flashes. *The units I, II and III are all built coaxially. Consequently they have very low inductance.*

Fig. 2 shows unit I. Five SIC condensers in series (10.5 kV and 0.1 μF each) are placed (by means of plastic holders) along the axis of a copper tube, 1.2 m in length. The X-ray flash tube is directly connected to the outermost condenser. The system is sketched in the upper part of the figure. The flash tube and part of the copper tube are seen in the lower part of the figure. E is the tube body which is also seen in Fig. 1. The system C + T (cathode and trigger electrode) is fastened to B by screwing on ring G. The trigger T is drawn towards the insulator ring H by means of spiral springs not shown in the figure. Screws in T, working against the insulator ring I make it possible to vary the distance between C and T. This trigger gap is about 0.3 mm. The connections between the porcelain insulator and the metal pieces D and Y are tightened with Araldit. The pieces R and Y are soldered together. At Z the flash tube is connected to the foremost condenser. The condenser battery and the anode are supplied with high voltage via the metal pin U. A resistance chain with 51 MΩ in parallel with each condenser guarantees a uniform voltage distribution over the condenser battery. The anode holder is water-cooled. In the figure the cooling system is only indicated by the water-supplying tubes T. The glass tube Q catches on its

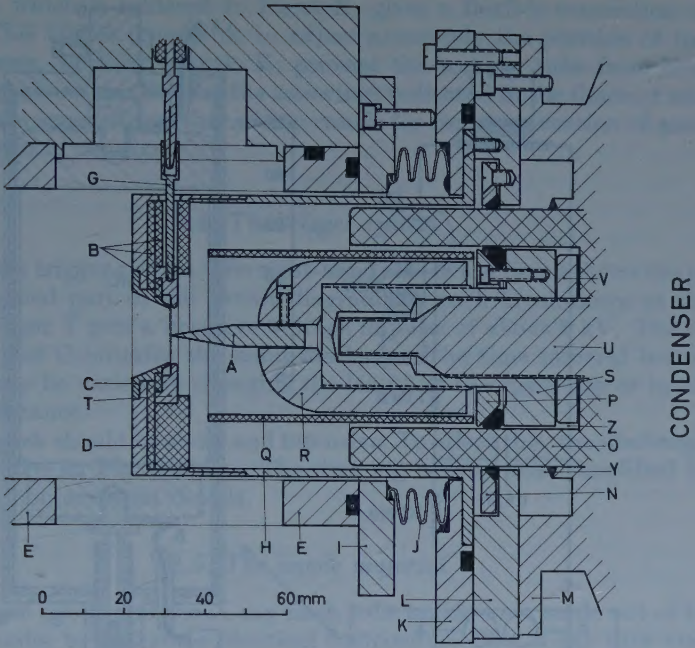

Fig. 4. Unit III. A = anode, C = cathode (of steel), T = trigger (of steel), B = three insulator rings of pyrophyllite, Q = glass tube, O = porcelain insulator, J = tombac tube. G, D, H, I, K, L, N, P, S, R, U and V are made of brass, M of iron. For further information, see text.

nner side metal vapor that comes from the anode point at every flash. If the glass tube is not used, a thin metal layer is rapidly formed on the inner side of the porcelain insulator, thus destroying the insulation. The thin copper ring L causes a certain elasticity of the connection between the spectrograph and the long copper tube. The following parts of the apparatus are screwed together (this is not shown in the figure): B and E, D and E, K and D, L and K, M and L.

Fig. 3 shows unit II. The condenser and the flash tube are rigidly built together. The condenser has extremely low inductance. It was constructed by Fil. lic. Robert Nilsson at this Institute. The condenser windings in the space W form a sequence of concentric coaxial cables. One pole is connected to the anode holder U and the other to the ring M. The brass envelope of the condenser serves as a return conductor. The electrode system C + B + T which is drawn on a double scale is attached to the brass tube E. The bellows S are used because of the thermal expansion of the oil. The pieces D, E, H, I and J are soldered together. K is fastened to J and M with screws. The connections between F and U, F and E, S and R, R and P, P and M are tightened with Araldit.

Fig. 4 shows unit III. The condenser and the flash tube are rigidly built together. The condenser (type CTU, 60 kV, 0,25 μF) is manufactured by ASEA. Its size is about $35 \times 35 \times 25$ cm^3. Fig. 2 in reference [8] shows a CTU condenser. Fig. 4 in the present paper shows the foremost part of the condenser: the envelope M, the porcelain insulator O and the bottom plate V with the threaded brass bolt U. ASEA originally intended to tighten the connections between the porcelain and the metal by soldering.

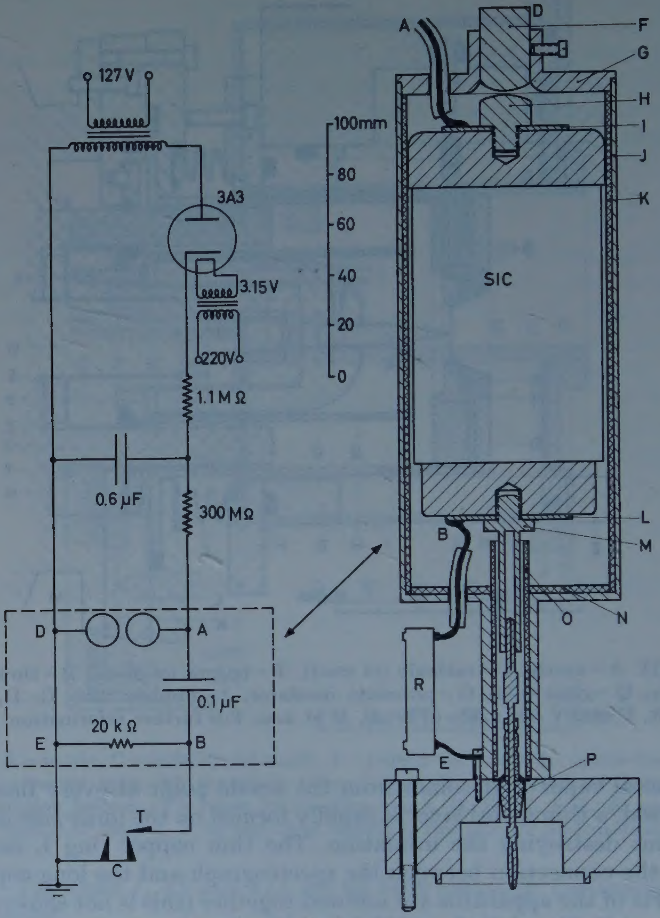

Fig. 5. The trigger system. C = cathode, T = trigger electrode. SIC = condenser of 10.5 kV and 0.1 µF, R = resistance of 20 kΩ. P = sealed terminal with two banana plugs. K, N and O are insulators of bakelite. F, G, H, I and J are made of brass.

This proved unsuccessful. To obtain perfect tightening ASEA used Araldit on both sides of the porcelain insulator (at Y and Z), besides the solderings. This brought new difficulties with it, however, when the condenser was used for high vacuum discharges. Residual gas from the Araldit material caused undersirable discharges and these often released more gas from the Araldit material, thus completely destroying the high vacuum. It was found necessary to shut in small air volumes nearest to the condenser on both sides of the porcelain insulator. As the figure shows, this was done by means of rubber packings pressed against the inner and outer sides of the insulator. This was troublesome, since the walls of the insulator were not quite circular-cylindrical in shape. However, this method was practicable. Consequently the inner side of the metal piece S (which is screwed on to the bolt U) is always under atmospheric pressure. The metal piece R is screwed on to S, thereby lowering the inductance. R is the anode holder. The glass tube Q catches the metal vapor from the anode point. The tombac tube J, which is soldered to I and K, gives a flexible connection with the spectrograph. This makes it possible to adjust accurately the position of the anode point. Stop screws, working against K, prevent the tombac tube from being compressed at the evacuation. Besides the screwings indicated in the figure, I and E and also C and D are screwed together. Some canals for rapid evacuation of screw-holes etc. are not shown in the figure.

2.4. *The trigger system*

Fig. 5 shows the trigger system. The right-hand side of the figure shows the practical shape of the framed part of the circuit diagram. At each break-down at the spark gap AD the trigger T gets a negative voltage impulse of about 8 kV. The resulting arc between T and C initiates the main discharge. The time interval between two trigger pulses may be varied by changing the length of the spark gap or by changing the 300 MΩ resistance.

The trigger spark should be short and intensive. To effect this, the discharge circuit was built coaxially, as Fig. 5 shows. The drawing is somewhat simplified but only with respect to non-essential details.

2.5. *The anode material*

The X-ray tube anode and the X-ray flash tube anode were made out of the same metal piece in order to guarantee identical composition. The X-ray tube anode was a plate of dimensions $18 \times 11 \times 2.0$ mm^3. The flash tube point of unit III had a top angle of only 20°.

The Fe material was Bofors B2V with about 99.95 % purity and with C as the main impurity element.

The Ni material had a guaranteed purity of > 99 % with the following impurities: Fe(< 0.40 %), Mn(< 0.35 %), Cu(< 0.25 %), Mg(< 0.20 %), C(< 0.15 %), S(< 0.01 %) and Si (< 0.15 %).

The Cu material was electrolytic copper with about 99.95 % purity.

2.6. *The microphotometer*

The photographic plates were studied with a Moll recording microphotometer, type A, Nr K15. The photometer lamp was supplied by a battery with good voltage constancy.

3. Experimental procedure

After bending, the crystal was tested both optically and by X-ray exposures. The radius of curvature was determined to 508 ± 1 mm and CD and PD in Fig. 1 were accordingly adjusted. Then the spectrograph was adjusted according to [7]. For each line to be studied, the position of the focusing circle was additionally controlled by exposing an inclined plate. For intensity reasons the distance FC in Fig. 1 was chosen as small as possible. (The size of the focus spot of the flash tube was the determining factor.) Consequently FC was 219 mm in all cases except when recording Fe $K\alpha_{1,2}$, when FC was 249 mm.

The free crystal face was 3.0 mm high and 11.5 mm wide. No special shutter was used. It was observed that a shutter that diminished the effective crystal breadth to 5.5 mm did not improve spectral resolution noticeably.

Screens arranged in different ways protected the photographic plate against light from the flashes and from the filaments of the vacuum-meter tubes etc. Furthermore, the plate was surrounded by a thin carbon paper. The X-ray absorption in the carbon paper was quite negligible. The absorption in the aluminum foil in the tube T in Fig. 1 was of the order of 10 % for the investigated lines.

The aim was to make the two types of exposures (X-ray exposure and X-ray flash exposure) under equal conditions.

The centres of the two focus spots were adjusted to the same position relative to the spectrograph. For unit III the accuracy of the vertical adjustment was ± 0.3 mm.

In both types of exposures the pressure was about the same. A special investigation showed that the pressure measured at Z in Fig. 1 might very well differ from the pressure in the X-ray tube (flash tube) by a factor of 2 or 3 with some small leak present in the system. In most exposures, however, the presssure was probably near 5×10^{-5} mm Hg.

The X-ray tube voltage was kept equal to the initial voltage of the flashes or a single kV or so higher. The voltage noise was ± 0.3 kV in ordinary exposures. Consequently the voltage during the X-ray flash was always lower than, or about equal to, the X-ray tube voltage. But this is not essential. Ordinary X-ray exposures with voltages between 14 and 50 kV did not show any variations of the line profiles investigated.

The time interval between the flashes was between 2 and 10 sec for unit I and about 17 sec for unit III. In the latter case the mean power was about 12 W and the mean temperature was low, despite the absence of any special cooling system. One consequence is that the anode point maintained its pointed shape even after 1000 flashes, though it was shortened about 2 mm by the action of the flashes. Each flash could be observed by means of a system of mirrors.

Typical values of voltage, number of flashes etc. are given in 4.1. From 4.1. it is also clear that unit III gives a dose (of the characteristic radiation) 3 or 4 times greater than the dose of unit I (at the same voltage). The ratio of the capacitance values is 12:1 and the ratio of the inductance values is 1:3.

It soon appeared that the investigated lines were broadened in the flash spectrum. In order to establish a weak broadening with the photographic method, it is necessary to compare plates with equal background and equal maximum density. With increasing maximum density, the apparent width of the line increases. When recording the $K\alpha_{1,2}$ lines, the apparent intensity ratio of these two lines changes with increasing maximum density. But if the demands for equal background and equal maximum density are fulfilled, then a satisfactory comparison is possible without the knowledge of the characteristic curve of the photographic plate. The efforts to expose on the same photographic plate an X-ray line above an X-ray flash line with the same background and the same maximum density were seldom successful. But this was no serious disadvantage, if only the plates were all developed and fixed in exactly the same way. This was done. In all cases the plate with the X-ray flash spectrum was compared to a plate with the ordinary spectrum with equal or negligibly higher photographic density.

The microphotometer was so adjusted that 1 mm on the photographic plate corresponded to 50 mm on the photometer paper. The recording of the microphotometer curve was made at the lowest rate. Since the widths of the slits of the microphoto-

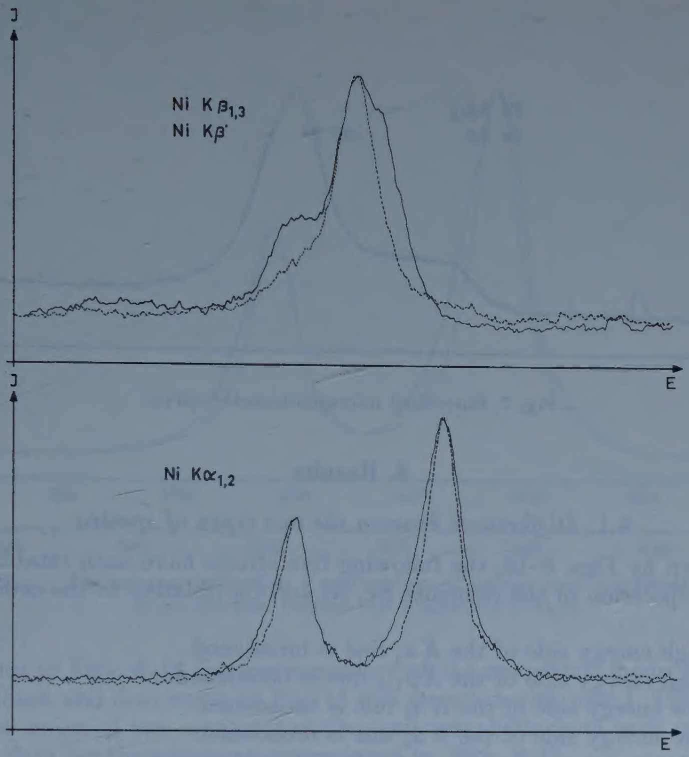

Fig. 6. Microphotometer curves. Photometer deflection I as function of spectral energy E. Solid line = X-ray flashes. Dotted line = ordinary X-rays.

meter influence the resolution in some degree, the same slit width was used for both spectra to be compared. As a rule, the slit dimensions were such that the illuminated region of the plate was 0.04 mm wide and 0.80 mm high.

Plates with the two types of spectra above each other were employed in determining energy shifts that might possibly occur. Microphotometer curves were recorded on the same photometer paper for five different levels of each line of the photographic plate. The tops of the photometer curves were arranged at regular spacings below each other on the photometer paper. Since the motion of the photometer paper is coordinated with the motion of the photographic plate, a straight line might be drawn through the five curve tops that correspond to one X-ray line on the photographic plate. The same is true of the five curves corresponding to the X-ray flash line. If there is no energy shift, the two straight lines on the paper will coincide. *In no case was an energy shift of the line top observed.*

The recorded photometer curves might be directly used for comparison (see Fig. 6). It was considered suitable, however, to correct for different background slopes. The curves were therefore smoothed, as Fig. 7 shows. At the same time correction was made for identified scratches on the plates. Point by point the smoothed curves were transferred to new diagrams which present a better picture of the magnitude of the observed effects (Figs. 8–13).

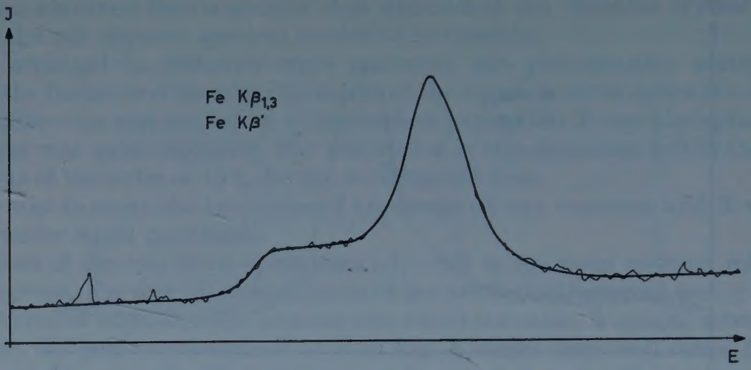

Fig. 7. Smoothed microphotometer curve.

4. Results

4.1. *Differences between the two types of spectra*

As is shown by Figs. 8–13, the following five effects have been established in the X-ray flash spectrum of the elements Fe, Ni and Cu (relative to the ordinary X-ray spectrum).

(1) The high energy side of the $K\alpha_1$ line is broadened.
(2) The high energy side of the $K\beta_{1,3}$ line is broadened.
(3) The low energy side of the $K\alpha_1$ line is broadened.
(4) The low energy side of the $K\alpha_2$ line is broadened.
(5) The relative intensity of the satellite $K\beta'$ is increased.

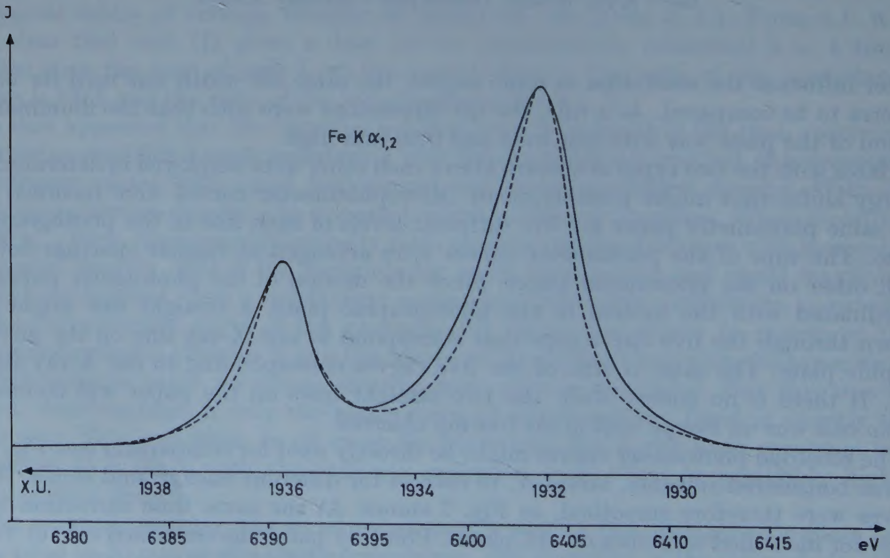

Fig. 8. Fe $K\alpha_{1,2}$. Photometer deflection I as function of energy and wavelength. Solid line = X-ray flashes. Dashed line = ordinary X-rays.

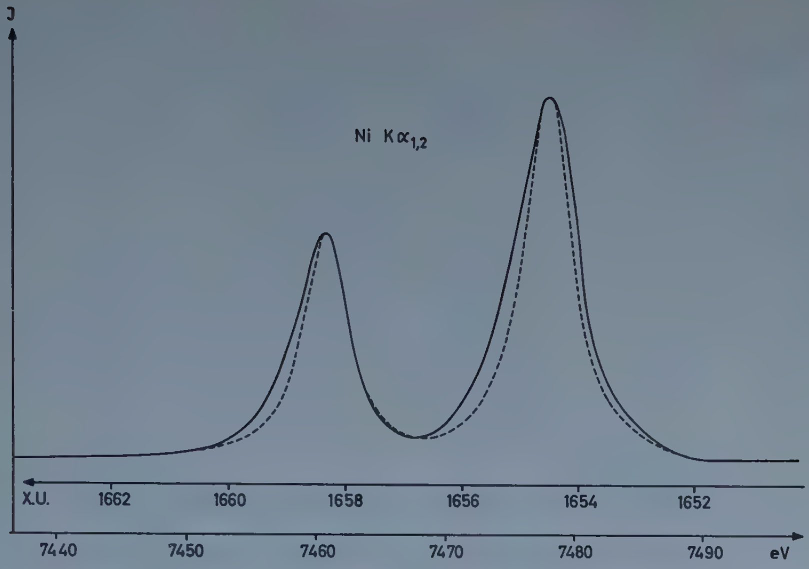

Fig. 9. Ni $K\alpha_{1,2}$. Photometer deflection I as function of energy and wavelength. Solid line = X-ray flashes. Dashed line = ordinary X-rays.

The curves in Figs. 8–13 are representative of the recordings made with unit III. The third (dash and dot) curve in Fig. 11 was recorded with unit I. The $K\alpha_2$ part of Fig. 8 is the mean of two curves that diverged very little from each other. Table 1 gives some data for the exposures represented by Figs. 8–13.

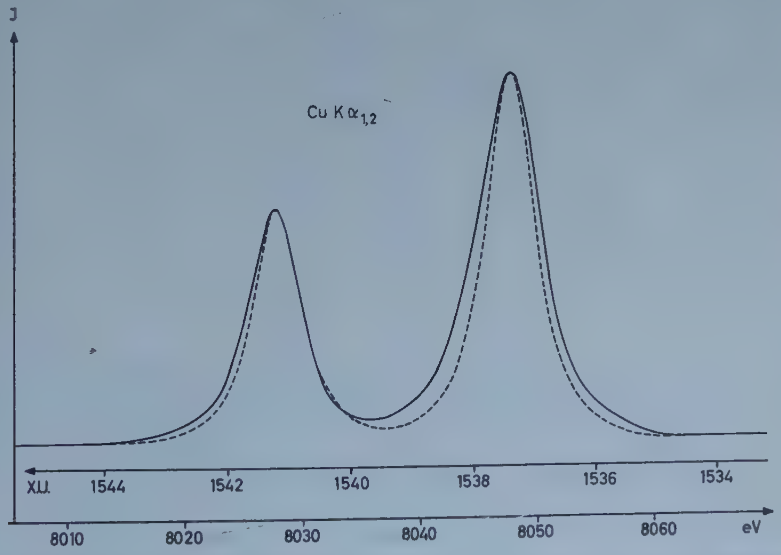

Fig. 10. Cu $K\alpha_{1,2}$. Photometer deflection I as function of energy and wavelength. Solid line = X-ray flashes. Dashed line = ordinary X-rays.

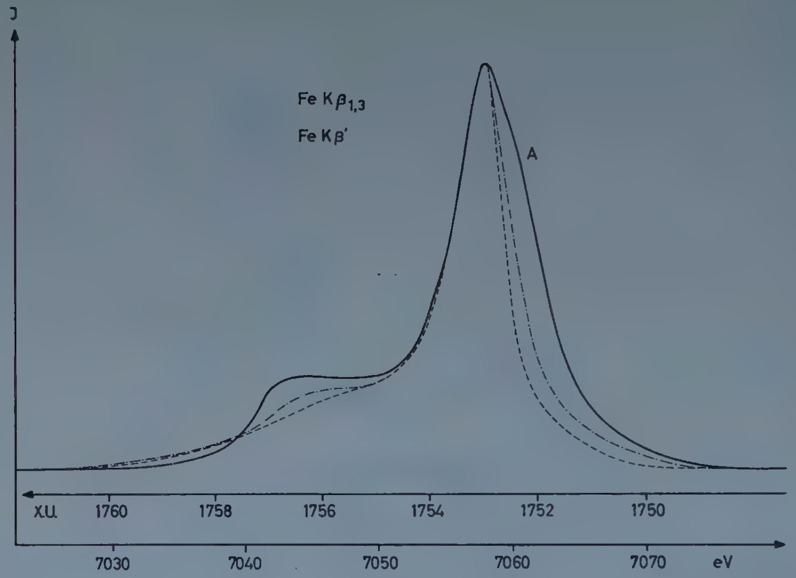

Fig. 11. Fe $K\beta_{1,3}$. Photometer deflection I as function of energy and wavelength. Solid line = X-ray flashes, unit III. Dash and dot line = X-ray flashes, unit I. Dashed line = ordinary X-rays.

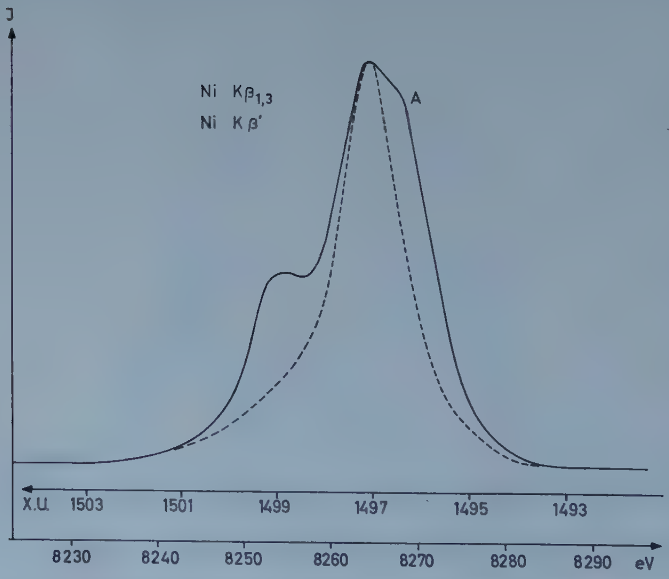

Fig. 12. Ni $K\beta_{1,3}$. Photometer deflection I as function of energy and wavelength. Solid line = X-ray flashes. Dashed line = ordinary X-rays.

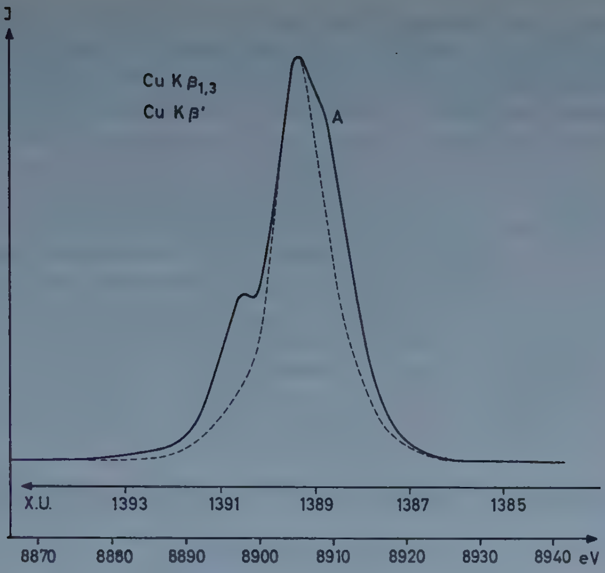

Fig. 13. Cu $K\beta_{1,3}$. Photometer deflection I as function of energy and wavelength. Solid line = X-ray flashes. Dashed line = ordinary X-rays.

Table 1.

Lines	Ordinary X-rays			X-ray flashes			
				Unit III		Unit I	
	Voltage kV	Current mA	Exposure mA × min	Voltage kV	Number of flashes	Voltage kV	Number of flashes
Fe K $\alpha_{1,2}$	44	2.5	2.5	41	370	46	~7000
Ni K $\alpha_{1,2}$	42	1.5	3	41	400		
Cu K $\alpha_{1,2}$	42	1.5	4	42	339		
Fe K $\beta_{1,3}$	47	3	14	43	1900		
Ni K $\beta_{1,3}$	42	2	12	42	842		
Cu K $\beta_{1,3}$	42	2	10	42	1000		

A recording of Fe $K\beta_{1,3}$ by means of unit II at 26 kV gave just the same magnitude of the observed effects as did a recording by means of unit I at 46 kV. The former recording is, therefore, well represented by the dash and dot curve in Fig. 11.

The observed effects were throughout much less when recorded by unit I than when recorded by unit III. Preliminary results of the present investigation were given in two conference reports [9, 10]. These reports concerned experiments with units I and II. Of the above-mentioned five effects, only the following effects were considered as established: (2) for Fe, (3) for Fe, Ni and Cu, (5) for Fe, Ni and Cu.

In Figs. 8–13 the lines to be compared have been given the same maximum intensity. This is somewhat arbitrary. This method is, however, the best, as long as we do not know more about the true form of the extra contributions in the flash spectrum.

Table 2 gives approximate values of the magnitude of each extra contribution. The values are calculated from Figs. 8–13 and are mean values for the three elements.

Table 2.

Line	Extra contribution in the flash spectrum	
	High energy side %	Low energy side %
K α_1	10	13
K α_2	0	10
K $\beta_{1,3}$	23	16

The effects recorded by means of unit I were smaller by a factor of about 3.

4.2. *The current density*

The focus spot of the X-ray tube was 10 mm². The current density at 3 mA is 3×10^{-4} A/mm².

The current density in the X-ray flash tube is much more difficult to estimate. The size of the focus spot was determined by means of a pin-hole camera. It was about 7 mm². However, the greatest current density probably prevails nearest to the point.

Formula (1) gives an approximate value of the maximum current during the discharge. The inductance of each discharge circuit was determined by an oscilloscope study of the oscillation period. Table 3 gives the inductance values and the calculated values of I_{max}.

Table 3.

Unit	L mμH	C μF	V_0 kV	I_{max} kA
I	254	0.0197	46	13
II	17	0.0449	26	42
III	84	0.248	43	74

The effective value of the current density is distinctly lower, of course. When the current has reached its maximum value, the tube voltage has decreased considerably. No attempt will be made here to estimate the effective value of the current density. We only note that $I_{max} = 74$ kA corresponds to a current density of about 1×10^4 A/mm².

5. Sources of error

Some factors are not the same in the two types of exposures: instantaneous values of voltage, current and X-ray dose rate, the temperature of the focus spot and the geometry of the focus spot.

The profiles of the investigated lines of the ordinary X-ray spectrum are quite the same for all the voltages of interest. Thus, the fact that the tube voltages differ does *not* in itself cause any difference between the two types of spectra.

The question arises if the very high X-ray dose rate during the flash is accompanied by a change of the characteristic curve of the photographic plate. Ehrlich and McLaughlin [11] have studied the characteristic curves of two conventional X-ray films as functions of exposure rate. The greatest exposure rate was of almost the same magnitude as the rate during the flashes. The exposure was then divided into portions of 10 μs separated by intervals of 0.6 s. Ehrlich and McLaughlin did not observe any reciprocity-law failure in the ascending branches of the characteristic curves. In the present investigation the maximum density of the plates was always fairly low. The fact that the X-ray dose rates differ is supposed *not* to introduce any error in the comparison of the two spectra. It should be observed, too, that a broadening effect caused by a reciprocity-law failure must be equally powerful on both sides of an X-ray line. Therefore, the observed effects cannot be ascribed to reciprocity-law failure.

As Parratt [12] points out, the temperature of the anode does not influence X-ray line widths considerably. Concerning the influence of the anode temperature on certain satellites see 6.3. In 6.3 it is also shown that a temperature increase of the order of 1200°K does not give an appreciable broadening of Fe $K\beta_{1,3}$.

The high temperature of the X-ray flash tube anode might possibly be accompanied by an enhanced risk of oxidation even at a pressure of 5×10^{-5} mm Hg. Sanner [13] has studied the shifts of $K\alpha_2$, $K\alpha_1$, and $K\beta_1$ for the oxidation processes $Cu \rightarrow CuO$, $Ni \rightarrow Ni_2O_3$, $Fe \rightarrow FeO$, and $Fe \rightarrow Fe_2O_3$. He did not find any shifts except for Fe $K\beta_1$ (+0.3 eV for $Fe \rightarrow FeO$ and +0.7 eV for $Fe \rightarrow Fe_2O_3$). Photo-electron measurements by Nordling, Sokolowski and Siegbahn [14] are in disagreement with Sanner's results and indicate a $K\alpha_1$-shift of $+1.9 \pm 1.3$ eV for $Cu \rightarrow CuO$. However, there is no accumulated oxidation or other contamination, for the anode point loses about 0.1 mg per flash of its surface layer. On the basis of these facts, it is concluded that oxidation or other contamination is *not* an appreciable source of error.

If the centres of the two focus spots do not coincide vertically, an error arises in the determination of the shifts. The maximum possible error is given by the following formula [7]:

$$b = \frac{h^2}{2\,(R \sin\theta + A)\cos\theta}, \tag{2}$$

where R is the radius of curvature of the crystal, A is the distance between the focus spot and the crystal, h is the vertical distance between the two focus spots and b is the error measured in length units along the photographic plate. With $R = 508$ mm, $A = 219$ mm, $\theta = 40°$ and $h = 0.3$ mm b will correspond to only 4×10^{-4} X.U., which is negligible.

The vertical extent of the focus spot causes a broadening on the low energy side of each line. This broadening may be calculated with the use of formula (2), if h means half the height of the focus spot. If the two focus spots have different h values, they will be unequally broadened. The vertical extent of the focus spot was 0.6 mm in the X-ray tube and about 0.7 mm in the X-ray flash tube. The resulting difference between the broadenings is completely negligible. This is also confirmed by the Fe $K\beta_{1,3}$ exposures. The satellite $K\beta'$ is there well separated from $K\beta_{1,3}$. The low energy side of the ordinary X-ray $K\beta_{1,3}$ profile was identical with the X-ray flash $K\beta_{1,3}$ profile.

There seems to be left only one factor as the posssible cause of the observed effects: the much higher current density of the X-ray flash discharge.

6. Interpretation

6.1. *The high energy side effects*

It is well known that, for instance, the transition $K \rightarrow L_{III}$ in an atom with only one inner vacancy gives a quantum with less energy than the $K \rightarrow L_{III}$ transition of an atom with more than one inner vacancy. Most X-ray satellites are supposed to represent electron transitions in multiply ionized atoms. Accordingly, most satellites are found on the high energy side of their parent line ($K\alpha_1$ in the above example).

The broadening on the high energy side of $K\alpha_1$ and $K\beta_{1,3}$ in the X-ray flash spectrum of the three elements is probably caused by *multiple ionization by successive collisions with incident cathode electrons.*

The X-ray flash line represents the sum of many different quanta with almost the same energy. They correspond to transitions partly in atoms that are singly ionized, partly in atoms that are multiply ionized in different ways. In many cases the extra vacancies may be situated in the outermost shells. The turn of the line profile observed at A in Figs. 11–13 is probably a consequence of the prevailing distribution of the different multiple-vacancy states.

The total broadening is greater for $K\beta_{1,3}$ than for $K\alpha_1$. This is quite natural. Extra vacancies in the outer shells should influence the energy of an M electron more than the energy of an L electron.

It is not clear why it has not been possible to establish a similar broadening on the high energy side of $K\alpha_2$. Some selection rules may possibly be operating with this result.

6.2. *The low energy side effects and Parratt's theory*

In 1959 Parratt published a work about the electronic band structure of solids, studied by the method of X-ray spectroscopy [12]. This is of great interest in connection with the present investigation. He points out that every X-ray transition is a multi-electron process. He criticizes the one-electron model and rejects the conventional energy level diagram as being incomplete. He proposes a new type of energy level diagram justified by the following arguments. In a K-excitation process the ejected electron may completely leave the atom or it may remain bound in an orbital outside the occupied valence orbitals. In this event the system is in one type of excitation state, called a bound-ejected electron excitation state. States of this type are supposed to be commonly produced in X-ray absorption but only rarely produced by bombardment with cathode electrons in an X-ray tube anode. When the K-state is produced, the change in the Hamiltonian of the system occurs in less than about 10^{-18} s, and in consequence of this change all the electrons are forced to change their wave functions. It is supposed that the inner electrons shift rather quickly to the respective new orbitals closer to the nucleus of the atom, but the valence electrons may require more time. The allotted time is about the lifetime of the inner vacancy, of the order of 10^{-16} s. At the termination of this time some of the valence electrons may have succeeded in following the new orbitals and the others may have been obliged to go to an unoccupied excitation orbital. In this event, the system is in a so-called valence-electron-configuration excitation state. It should be observed, too, that the cathode electron that produces the K-vacancy may also eject one or two outer electrons. The conclusion is that a K-vacancy may be associated with *many* different electron configurations and, consequently, with *many* different energy levels. A satisfactory energy level diagram with the energy of the quite unexcited system as zero level must have not *one* but *many* K-levels. Analogously there must be many L_{I}, L_{II} and L_{III}-levels, etc. The probability is often low, however, for all but one state within each group of states. It is believed, for instance, that for many solids the $K\alpha_1$ line from a conventional X-ray tube represents the single transition $K_\tau \rightarrow L_{\mathrm{III}\tau}$. The K-level marked K_τ refers to the electron configuration in which, conventionally, the K electron has been removed to "infinity" in the solid and left there with zero kinetic energy. Of course, a similar state exists for L_{III}-vacancies etc. For some materials, e.g., solids having s-type valence electrons and an incomplete inner shell (transition metals), the $K\alpha_1$ line is supposed *not* to be represented by the single transition $K_\tau \rightarrow L_{\mathrm{III}\tau}$. Other states with "abnormal" configurations of the valence electrons are believed to be important, too.

This question was studied more closely in a later paper by Skolnick and Parratt [15]. They present calculations for the K spectrum of solid metallic manganese. They show that Parratt's multi-electron model is able to explain satisfactorily the observed asymmetries of the $K\alpha_{1,2}$ lines and the origin of $K\beta'$ for elements of the first transition group. The lines $K\alpha_{1,2}$ and $K\beta_{1,3}$ themselves are supposed to represent transitions in atoms where the $4s$ electrons have *not* adjusted themselves to the new Coulomb field when the K-vacancy is filled. The low energy surplus of $K\alpha_1$ and $K\alpha_2$ and the satellite $K\beta'$ on the low energy side of $K\beta_{1,3}$ are supposed to represent mainly transitions in atoms where the 4s electrons *have* adjusted themselves to the new field and are more strongly bound.

According to some earlier theories, the origin of $K\beta'$ is one of the following alternatives: (*a*) a two-electron transition $KL_{\mathrm{II,\,III}} \rightarrow L_{\mathrm{I}} M_{\mathrm{IV,\,V}}$ [16], (*b*) Compton and Raman scattering of the $K\beta_{1,3}$ doublet in the X-ray tube anode [17], or (*c*) splitting of the X-ray state as a result of angular momentum coupling between the K-vacancy and the incomplete $M_{\mathrm{IV,\,V}}$ shells [18], [19]. These three theories are rejected by Parratt for the following reasons, respectively: (*a*) the transition probability is too low, (*b*) similar components are not observed for other lines, for instance $K\alpha_{1,2}$, and (*c*) the splitting cannot possibly be strong enough.

Skolnick and Parratt point out that, with an increasing degree of multiple ionization, the 4*s* electrons will have a tendency to readjust more easily to the new Coulomb field. This means that with increasing multiple ionization the intensity of the low energy components of $K\alpha_1$ and $K\alpha_2$ and the intensity of $K\beta'$ should increase. *The present results seem to support Parratt's theory.*

Skolnick and Parratt also point out that with an increasing degree of multiple ionization the energy difference between the high energy component and the low energy component should increase. In this respect the present investigation gives only a faint indication in the direction predicted by Skolnick and Parratt. This is illustrated in Table 4, which gives the $K\beta'$ wavelength according to some earlier measurements [20–22] and the wavelength of the maximum of the additional low energy contribution in the X-ray flash spectrum. Data are given for the spectra recorded by unit I and those recorded by unit III (with the greatest current density).

When Table 4 is studied, it should be remembered that $K\beta'$ is broad and diffuse, and that the accuracy of the photographic method is comparatively low. However, realizing that the high energy component to be associated with the additional low energy contribution has an energy higher than that of the ordinary $K\beta_{1,3}$ line, we must conclude that the present wavelength measurements constitute a (weak) support of the theoretical predictions.

Table 4.

Wavelength in X.U. for	Fe	Ni	Cu
K β' according to [20]	1756.0		1390.7
K β' according to [21]	1756.48	1499.48	
K β' according to [22]	1756.46	1499.10	
Additional contribution, unit I	1756.5	1499.1	1390.7
Additional contribution, unit III	1756.8	1499.1	1390,7

Generally Cu is not considered to be a transition element. In the X-ray flash anode, however, extra vacancies are occasionally created in the 3*d* shell, and then Cu should have transition element character.

6.3. *The low energy side effects and Kakuschadse's theory*

In 1959 Kakuschadse published a theoretical work [23] about some of the X-ray satellites of the transition metals. Kakuschadse attempts to explain the satellites $K\alpha_3$ and $K\beta'$ as well as the asymmetry of $K\alpha_1$ and $K\alpha_2$ as a result of interaction between the electrons and the lattice vibrations. The three satellites $K\beta'$, $K\alpha_3$ and No. 6 (Fig. 14) are all supposed to represent two-electron transitions. According to Kakuschadse, the origin of $K\beta'$, for instance, is the double transition $K \rightarrow M_{\mathrm{II,\,III}}$ plus $N_{\mathrm{I}} \rightarrow M_{\mathrm{IV,\,V}}$. At $K\alpha_2$ there exists a satellite corresponding to No. 6.

Kakuschadse gives a theoretical expression for the relative intensity of $K\beta'$. According to this expression, the relative intensity is strongly temperature-dependent: at 400°K ~ 20 %, at 700°K ~ 50 % and at 1200°K strongly predominant over the parent line $K\beta_{1,3}$.

Since the mean temperature of the emitting X-ray flash tube anode is higher than that of the emitting X-ray tube anode, the increased relative intensity of $K\beta'$ in the flash spectrum might be a temperature effect, if Kakuschadse's theory is valid.

In order to test this theory the following experiment was made. Fe $K\beta_{1,3}$ and $K\beta'$ were recorded both at a low temperature and at a high temperature of the X-ray tube anode.

In the low temperature experiment the anode was strongly water-cooled. The exposure was divided into portions of 10 s separated by intervals of one or two minutes. The current was low: 0.20 mA. The temperature rise ΔT during the exposure was estimated by means of the following formula which is valid for the centre of the focus spot and for short times of exposure [24, 25]:

$$\Delta T = \frac{2}{\sqrt{\pi}} \cdot \frac{Q \cdot \sqrt{t}}{\sqrt{\lambda c \varrho}}, \tag{3}$$

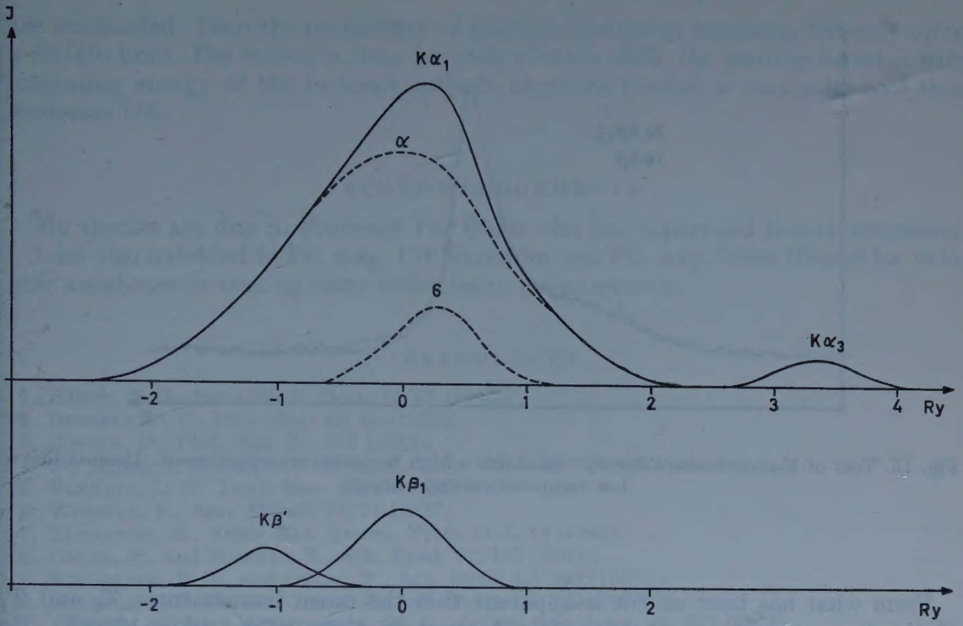

Fig. 14. The lines $K\alpha_1$ (including the satellite No. 6) and $K\beta_1$ and the satellite lines $K\alpha_3$ and $K\beta'$, according to Kakuschadse.

where $Q = \mathrm{V}\cdot\mathrm{I}/A$, λ is the thermal conductivity, c the heat capacity per gram and ϱ the density of the anode material, t is the exposure time, V is the voltage, I is the current and A is the area of the focus spot. With $\sqrt{\lambda c \varrho} = 0.384$ cal deg^{-1} cm^{-2} sec$^{-1/2}$ (a reasonable mean value for the temperature interval 20°–200°C), V $= 42$ kV, I $=$ 0.20 mA, $A = 10$ mm^2 and $t = 10$ s, formula (3) gives $\Delta T = 186°$. Consequently, the mean temperature during the exposure was $T_1 \approx 294 + \frac{2}{3} \times 186 \approx 420$°K.

In the high temperature experiment no water-cooling was used. At first the anode was heated for 240 s with V $= 42$ kV and I $= 3.50$ mA. Immediately after that, the exposure was made for 120 s with unchanged voltage and current. After the exposure it was observed that in the central part of the focus spot the melting-point $T_m \approx$ 1800°K had been attained. Formula (3) cannot be used for determining the temperature. With $t = 360$ s and I $= 3.50$ mA and with all the other quantities unchanged, formula (3) gives a final temperature of about 20,000°K (if the melting and evaporating processes are neglected). Since melting had just started, it is apparent that, with the exposure times used, the temperature rises much more slowly than is indicated by equation (3). Another consequence of this is that the estimated value of the mean temperature T_1 in the low temperature experiment might be too high. It is possible to get a lower limit of the mean temperature T_2 during the high temperature experiment in the following way. The temperture rise ΔT is supposed to obey the law

$$\Delta T = C \cdot \sqrt{t}$$

where C is a constant determined by the condition that $t = 360$ s gives a final temperature of about 1800°K. This gives an initial temperature of about 1520°K and a mean temperature T_2 of about 1670°K.

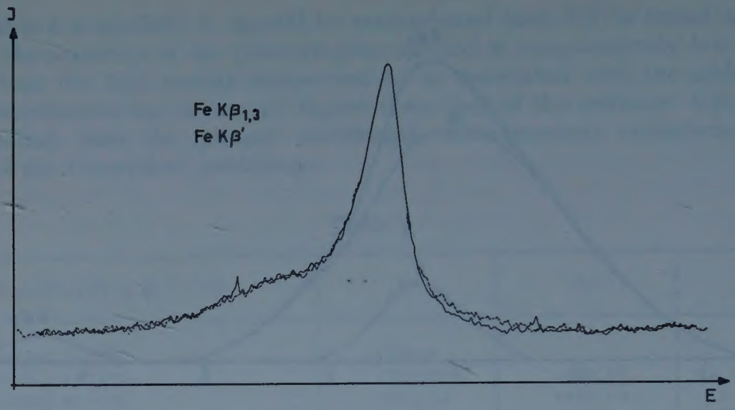

Fig. 15. Test of Kakuschadse's theory. Solid line = high temperature experiment. Dashed line = low temperature experiment.

From what has been said it is apparent that the mean temperatures T_2 and T_1 of the two exposures probably differed by more than $1670 - 420 = 1250$°K. No change of the relative intensity of $K\beta'$ was observed, however (see Fig. 15). *This result is quite incompatible with Kakuschadse's theory.* At exposures with mean temperatures between T_1 and T_2, the recorded photometer curves were also of the same shape as those of Fig. 15.

Further arguments may be given against Kakuschadse's theory. In the X-ray flash spectrum the $K\alpha_1$ line was broadened on the low energy side in the way shown in Figs. 8–10 but its maximum point was not displaced. It seems difficult to understand how this might be the result of a change of the relative intensity of the No. 6 line (Fig. 14) and a change of its energy separation from the α line.

One fundamental point in Kakuschadse's theory is the assumed magnitude of the mean time between the creation of a K-vacancy and a subsequent transition $K \to L_{\mathrm{III}}$, $\tau_{\alpha_1} \gtrsim 10^{-12}$ s. The present author proposes a different value; $\tau_{\alpha_1} \approx 3 \times 10^{-15}$ s. This is a value calculated from known data concerning the lifetime of a K-vacancy [12], the fluorescence yield [12], and the relative intensities of the X-ray lines.

6.4. *The voltage dependence of the observed effects*

The probability of multiple ionization should depend not only on the current density but also on the energies of the incident cathode electrons. As was mentioned earlier, unit II with $V_0 = 26$ kV and unit I with $V_0 = 42$ kV gave equal effects despite the greater current density in the former case.

Suppose that the current density is changed while all other factors are unchanged. With increasing current density the effects observed in the present investigation will increase. Finally multiple ionization before the X-ray transition will be a rule and single ionization will be an exception.

Suppose that the mean energy of the incident cathode electrons is successively increased (starting from low values) while all other factors, including current density, are unchanged. Then the probability of multiple ionization increases, but only up to a certain limit. The reason is that, for each electron shell, the ionizing function with increasing energy of the incident cathode electrons reaches a maximum and then decreases [26].

ACKNOWLEDGEMENTS

My thanks are due to Professor Per Ohlin who has supervised this investigation. I am also indebted to Fil. mag. Ulf Karström and Fil. mag. Sture Händel for valuable assistance in making some preliminary measurements.

REFERENCES

1. Hirsh, F. R., Revs. Mod. Phys. *14*, 45 (1942).
2. Rosseland, S., Phil. Mag. *45*, 65 (1923).
3. Coster, D., Phil. Mag. *44*, 546 (1922).
4. Du Mond, J. W. M., and Hoyt, A., Phys. Rev. *36*, 799 (1930).
5. Parratt, L. G., Phys. Rev. *49*, 132 (1936).
6. Wisshak, F., Ann. Physik *28*, 71 (1937).
7. Flemberg, H., Arkiv Mat. Astron. Fysik *28 A*, 18 (1942).
8. Ohlin, P., and Händel, S., Ark. Fysik *17*, 157 (1960).
9. Schörling, P. O., and Ohlin, P., Ark. Fysik *13*, 285 (1958).
10. Schörling, P. O., and Ohlin, P., Ark. Fysik *16*, 520 (1960).
11. Ehrlich, M., and McLaughlin, W. L., J. Opt. Soc. Amer. *46*, 797 (1956).
12. Parratt, L. G., Revs. Mod. Phys. *31*, 616 (1959).
13. Sanner, H., Thesis, Uppsala (1941).
14. Nordling, C., Sokolowski, E., and Siegbahn, K., Ark. Fysik *13*, 483 (1958).
15. Skolnick, M. H., and Parratt, L. G., Line asymmetry and satellites in X-ray spectra: Excitation states (1959).
16. Sawada, M., Sci. Mem. Kyoto Imper. Univ. *A 15*, 43 (1932).
17. Bloch, F., Phys. Rev. *48*, 187 (1935).
18. Parratt, L. G., Phys. Rev. *50*, 1 (1936).
19. Coster, D., and Druyvesteyn, J. M., Z. Physik *40*, 765 (1927).
20. Bearden, J. A., and Shaw, C. H., Phys. Rev. *48*, 18 (1935).
21. Ford, O. R., Phys. Rev. *41*, 577 (1932).
22. Eriksson, S., Z. Physik *48*, 360 (1928).
23. Kakuschadse, T. I., Ann. Physik *3*, 352 (1959).
24. Schaaffs, W., *in* Encyclopedia of Physics *30*, 15 (1957).
25. Schall, R., Z. angew. Phys. *2*, 83 (1950).
26. Massey, H. S. W., and Burhop, E. H. S., Electronic and Ionic Impact Phenomena. Oxford University Press, London (1952).

Tryckt den 30 januari 1961

Uppsala 1961. Almqvist & Wiksells Boktryckeri AB